STUDIES OF THE EFFECT OF 2ND HARMONIC ON THE E-P INSTABILITY AND RF CONTROL OF INSTABILITIES *

V. Danilov#, Z. Liu, ORNL, Oak Ridge, TN, U.S.A.

Abstract

The dependence of the electron–proton instability threshold on the 2nd harmonic voltage and on the longitudinal profile in general is observed in the Spallation Neutron Source ring. Possible explanations of this phenomenon are discussed in the paper. The most optimal RF configuration to mitigate instabilities is presented.

INTRODUCTION

The Spallation Neutron Source (SNS) Ring was designed and optimized for very intense beams with the number of protons above 10^{14} per pulse. Once this intensity was reached, a few instabilities were observed [1], with the electron-proton (e-p) instability being the strongest. This instability depends on accumulation of electrons in the vacuum chamber, which, in turn, depends on the longitudinal beam distribution. There are many papers on this subject (see, e.g. [2]), and the identified mechanisms of accumulation for long proton bunches are separated into two classes: single pass and multipass accumulation (see, e.g. [2]). They are often interrelated, but we believe the first one is the main source of electron production in the SNS ring. In our paper we focus on the single pass accumulation and its dependence on the longitudinal beam distribution.

SINGLE PASS ELECTRON ACCUMULATION AND ITS DEPENDENCE ON THE BEAM DISTRIBUTION

The main process leading to large density electron accumulation is secondary emission of electrons from charged particles accelerated in the electric field of the proton beam. Predominantly, those particles are electrons from residual gas in the vacuum chamber, electrons scraped from the vacuum chamber by lost protons, etc. The yield is measured and described in many papers. Here we present a fit to the yield as a function of incident electron energy from [3]. Figure 1 shows the dependence of true secondary electron yield versus energy of the incident electrons with zero incident angle on stainless steel (SS) and titanium nitrate (TiN) coated SNS vacuum chambers (most of the SNS vacuum chamber in the ring is coated with TiN). The maximal yield is larger for the stainless steel but in our regions of interest of energies around 100 eV they almost coincide.

*Research sponsored by Laboratory Directed Research and Development Program of Oak Ridge National Laboratory, managed by UT-Battelle, LLC, for the U. S. Department of Energy under Contract No. DE-AC05-00OR22725.

#danilovs@ornl.gov

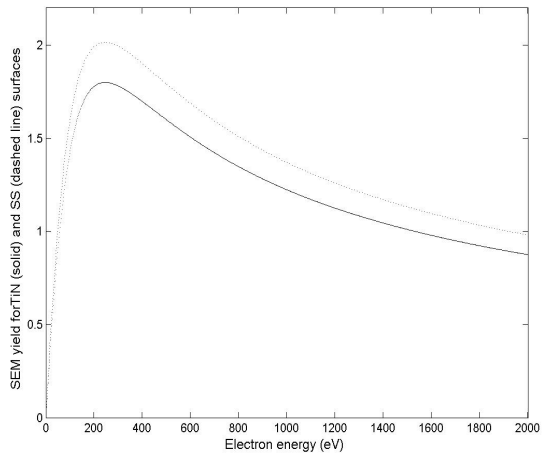

Figure 1: Secondary emission yields for stainless steel (dashed line) and titanium nitrate SNS coating (solid line) as a function of energy of incident electrons.

Most of the electrons due to secondary emission are generated at the trailing edge of the proton beam. The reason for this is simple – electrons near the walls of vacuum chamber are attracted by the proton beam as it passes by. Since the density of the beam is decreasing, the electrons are accelerated more during their pass into the beam than they are decelerated during their pass out of the beam. The resulting effect is that they acquire a rather large energy, and when they strike the opposite side of the wall there is enough energy to produce more than 1 electron on average per one strike.

The SNS maximum intensity ring beam can be approximated as a beam with $N=1.4\cdot10^{14}$ protons, a longitudinal distribution represented by an equilateral triangle with a trailing edge duration of 300 ns, and a round transverse distribution with r.m.s. radius 1 cm. The vacuum chamber radius is 10 cm. The incident electron energies at the trailing edge for these beam parameters range from 60 eV at the center of the beam, when the trailing edge begins, to 220 eV at the end. For the SNS chamber the yield for these energies ranges from 1 to 1.75.

More important is to find the average number of electrons, produced by one electron at the center of the beam, or the average trailing edge yield. We plot it as a function of the trailing edge slope (in this paper we always use linear longitudinal density of the trailing edge to make our estimates). It can be made longer or shorter by changing the 2nd harmonic RF in the SNS ring and for the same intensity and triangular (but lopsided) distribution it can vary from 0.5 to infinity in units of length of the trailing edge for a symmetric triangular distribution with the same total length.

Figure 2 shows the integrated yield for the SNS parameters as a function of trailing edge duration. In order to be consistent with the measurements shown below we have taken the intensity as $1.1 \cdot 10^{14}$ protons per pulse and have used a stainless steel chamber. The parameter *s* here is the trailing edge steepness which we define as 200 ns divided by the duration of the trailing edge.

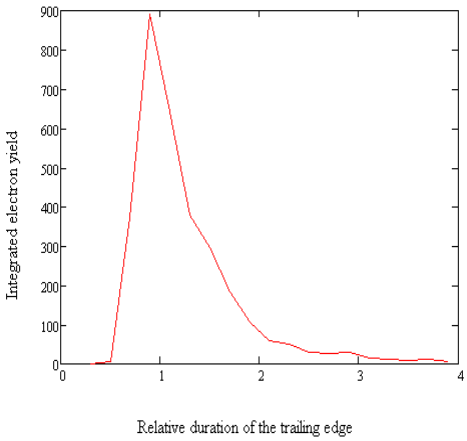

Figure 2: Stainless steel integrated yield as a function of trailing edge steepness *s*

One can see that it has sharp maximum around 1 and both short and long edges are good for cleaning up electrons. We don't show the same figure for TiN coated chamber since we don't see any substantial electron signals from the electron detector at these locations. We suspect that even the SS chambers don't produce many electrons (we have a few pieces of SS chamber). In addition, we have a few places (especially near the stripper foil) where the aluminium might be evaporated, as well as ceramic breaks of the vacuum chamber, bellows, etc., which may have larger secondary emission coefficients. We believe these places are most responsible for electron cloud generation. Figure 3 shows the integrated yield for aluminium. One can see that the integrated yield is an order of magnitude larger than that of the SS chamber in Fig. 2, and it is shifted substantially toward smaller *s*.

EXPERIMENTAL DATA

Now we are in a position to briefly analyze a collection of data taken in the SNS ring in the summer of 2009. We show here only the most representative data. The SNS Ring RF system consists of 3 first harmonic cavities, and one second harmonic cavity. By varying the phase of the second harmonic and the first harmonic amplitudes we were able to produce longitudinal distributions with various shapes and trailing edge slopes. Figure 4 shows a waterfall plot of the longitudinal distributions of beam taken from a Beam Current Monitor. Each line shows 2 turns of beam with a duration of 1 microsecond for each turn.

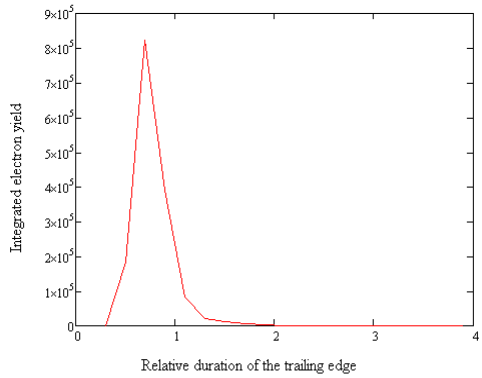

Figure 3: Integrated yield for aluminium as a function of parameter *s*.

The distributions are taken with increment 80 turns with the lowest intensity starting from the bottom. The total number of turns is around 1000. The RF 1st harmonic voltage was around 10 kV for two RF stations (one of them was off). Their phases were constant and equal to zero, meaning zero voltage at the center of the bunch. The 2nd harmonic RF amplitude was constant and was equal to around 15 kV, and its phase was -5 degrees. The chromaticity was natural, and the total number of protons per bunch was $1.1 \cdot 10^{14}$. One can see that this setup led to asymmetric distribution and a long trailing edge (the steepness parameter $s \approx 0.7$) that corresponds to the worst case of electron accumulation according to Fig. 3.

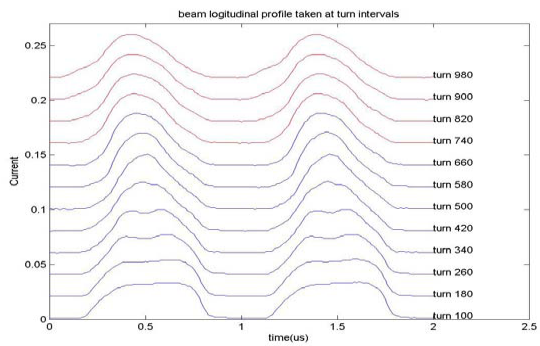

Figure 4: Progression of longitudinal distribution in the SNS ring. Each plot from the bottom up shows the distribution from the very beginning to the end with increments of 80 turns.

Indeed, this setup produced very strong e-p instability at the end of accumulation. Figure 5 displays a horizontal Beam Position Monitor (BPM) signal. One can see that in the last hundred 200 (the extraction of the beam in this figure corresponds to 1300 turns) turns of accumulation the signal grows rapidly 4 times above the noise level.

The vertical signal, not presented here, shows the same trend.

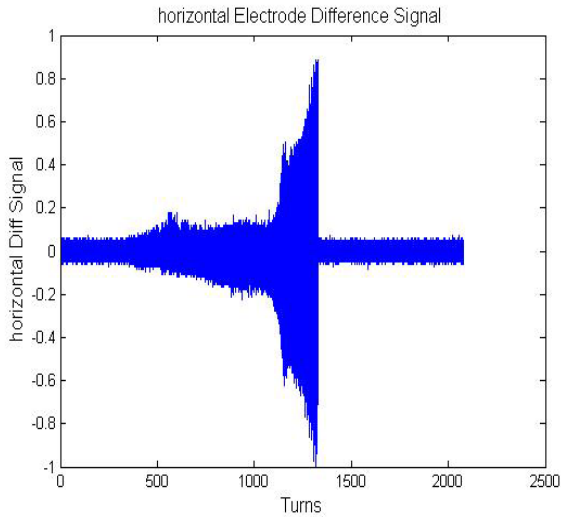

Figure 5: Instability signal from horizontal BPM.

Figure 6 shows the spectrum of the signal from Fig. 5 for each turn from 200 to 980 turns. The instability appears roughly 200 turns before the end of accumulation and spans the range of frequencies from 20 to 80 MHz.

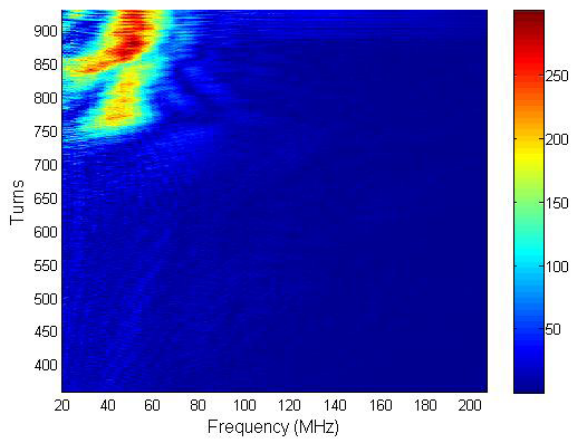

Figure 6: Power spectrum of the horizontal e-p instability. The horizontal axis is the frequency in MHz, and the vertical axis is time in units of 1 turn.

By reducing the 1st harmonic two cavities voltages to 5.5 kV and changing the phase of the 2nd harmonic RF station to -15 degrees we managed to produce an almost flat distribution with a steep trailing edge. Other parameters were kept the same. Figure 7 shows the longitudinal distributions during the process of beam accumulation in the ring. One can see that it is substantially different from Fig. 4.

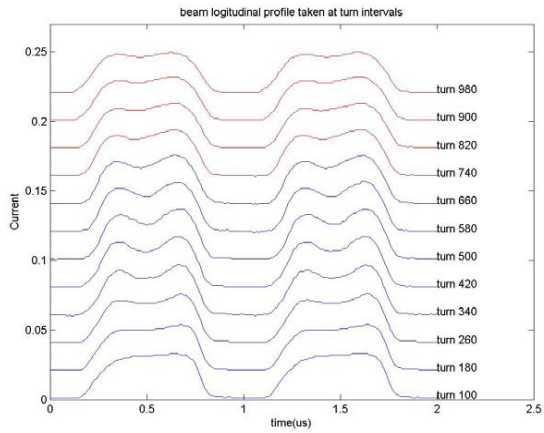

Figure 7: Progression of the flat longitudinal distribution in the SNS ring (the units and notations are the same as in Fig. 4).

The trailing edge steepness parameter was $s \approx 1.4$, and one can see from Fig. 3 that the integrated electron yield drops to almost zero at this value of s. Figure 8 shows the horizontal BPM signal for this beam. One can see that the signal barely appears from the noise and, as its analysis shows, some growth of the signal during accumulation is attributed to revolution harmonics rather than betatron oscillations (they are always present in the signals due to nonzero displacement of the beam at BPM locations).

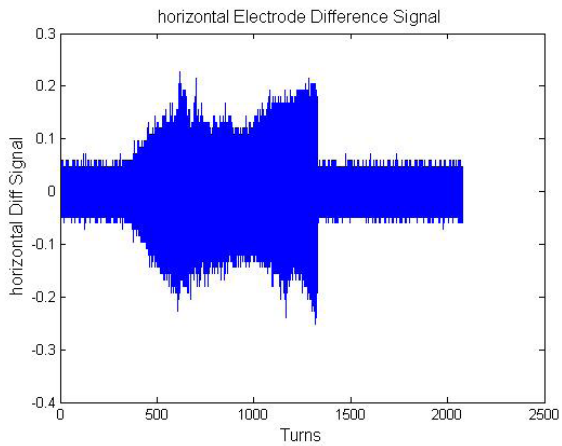

Figure 8: Instability signal from horizontal BPM for the flat beam.

Figure 9 shows the spectrum of the signal above. It doesn't show signs of e-p instability for the same intensity as before. One can argue that the RF configuration influences the energy spread of the beam, and this, in turn, changes the Landau damping. Therefore it is reasonable to separate these factors and measure them separately. We can say here (in support of our view that the secondary emission yield dependence on longitudinal distribution is dominant) that the most stable case had minimum RF voltage of the 1st harmonic, and, consequently, had the minimum energy spread, because at the end of SNS injection most of the spread is coming from transfer of longitudinal coordinate into the energy in the longitudinal phase space.

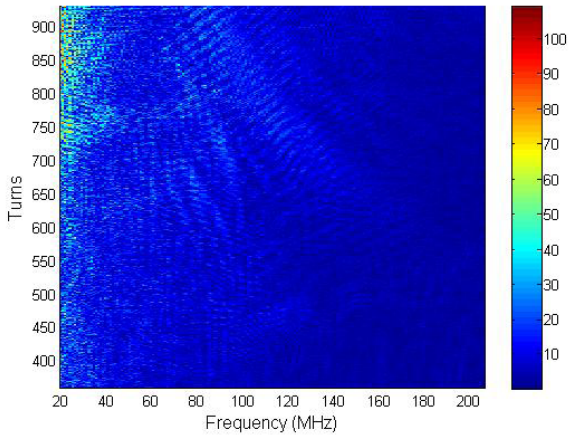

Figure 9: Power spectrum of the Fig. 8 signal.

BEST RF CONFIGURATIONS TO MITIGATE E-P INSTABILITY

Here we would like to elaborate on the nature of the dependencies of the integrated SEM yield as a function of the trailing edge steepness for the SNS parameters. Both Figures 2 and 3 have the same trend in behaviour of this parameter versus steepness *s*. Near its zero the integrated yield is very small because electrons have a very small acceleration and a small net energy gain after traversal of the proton beam. Figure 1 shows that the SEM yield is near zero for small energies. As the steepness increases, the SEM yield becomes larger than 1 and the integrated yield starts to grow until it reaches its maximum. The maximum is determined by two factors, namely, how many times the electrons strike the wall during one proton beam passage, and their energies. The first factor starts to drop rapidly with steepness grows, and the SEM yield starts to decrease with the energy after 200 eV (see Fig. 1). Therefore, the integrated yield starts to decline after some steepness parameter *s0*, which is around 1 for the SS chamber and 0.7 for the aluminium chamber for the SNS case. According to the above observations, there are two methods to reduce the electron production.

The first one is to decrease the steepness, but all we can do is to reduce it by factor 2 roughly – we have to make a very sharp leading edge of the beam and a long trailing edge, the duration of which, for a triangular distribution, can be only doubled. This factor 2 can obviously help, but it is not known whether we can create it in the SNS ring.

The other method to reduce the integrated yield is to increase the steepness *s*. In our experiments we reached a value of almost 1.5, and it helped to eliminate the instability for number of particles $N=1.1\times10^{14}$. For larger intensities, needed for the SNS Power Upgrade, we are afraid this won't be enough to cope with the instability. Probably, the best way to reduce it is to increase the steepness *s* by a factor 5. This is possible by introduction of a barrier cavity. It was already proposed a few years ago by one of the authors of this paper (V. D.). The SNS Ring dynamics was simulated later [4] and showed promising results not only for the electron accumulation, but also for a reduction in space charge effects. The SNS second harmonic is already very helpful in mitigation of e-p instability, and a natural evolution of this approach leads us to a barrier cavity and a sharp edge distribution. For the SNS Ring it is a perfect electron "killer" – electrons accelerated at the trailing edge ("single pass" electrons) acquire energy of the order of a few keV, where the SEM yield is less than 1 and, in addition, they die in the gap with only a small percentage survival rate. Electrons in the gap, accelerated by sharp edge barrier cavity distribution, again have a few keV energy, and are rapidly (not adiabatically) exit the proton beam at the trailing edge and are reduced significantly in density as well as "single pass" electrons. Therefore, in either way, electrons are subject to very rapid "cleaning" when interacting with the "barrier cavity" distribution having very sharp edges.

CONCLUSION

It is found experimentally that the e-p instability in the SNS ring depends strongly on longitudinal beam distribution. Possible explanations of the phenomenon are presented in the paper. In addition, best RF configurations to mitigate the instability, are discussed.

ACKNOWLEDGMENTS

The authors are grateful to the SNS accelerator physics team for numerous discussions and support.

REFERENCES

[1] V. Danilov, S. Cousineau, A. Aleksandrov, S. Assadi, W. Blokland, C. Deibele. S. Henderson, J. Holmes, M. Plum, A. Shishlo, "Accumulation of High Intensity Beam and First Observations of Instabilities in the SNS Accumulator Ring", 39th ICFA Advanced Beam Dynamics Workshop On High Intensity High Brightness Hadron Beams, Tsukuba, Japan, May-June (2006).

[2] V. Danilov, A. Aleksandrov, M. Blaskiewicz, J. Wei, "Calculations of the Electron Accumulation in the SNS storage Ring", PAC 2001, Chicago, USA, June 2001.

[3] M.T.F. Pivi and M. A. Furman, "Electron Cloud Development in the Proton Storage Ring and in the Spallation Neutron Source", PRST-AB, **6**, 034201 (2003).

[4] J.A. Holmes, S.M. Cousineau, V.V. Danilov, and A.P. Shishlo, "RF Barrier Cavity Option for the SNS Ring Beam Power Upgrade", HB 2006, Tsukuba, Japan, May-June, (2006).